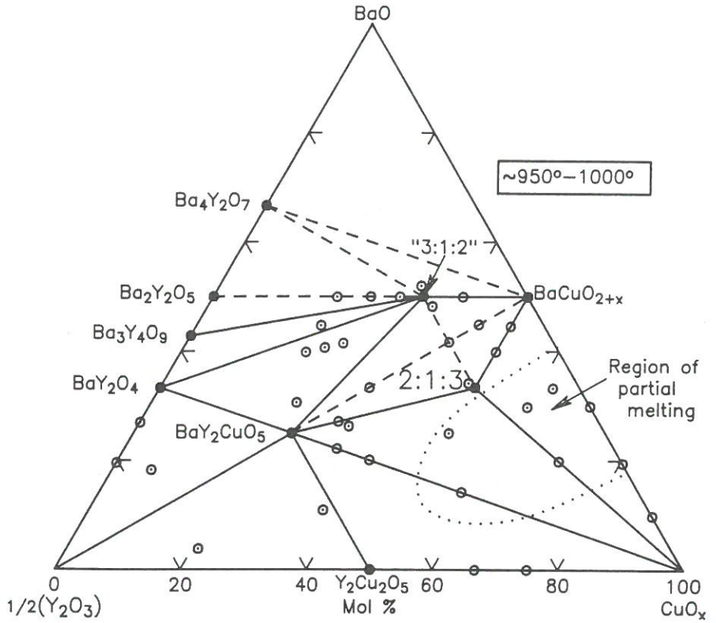

Figure 4 Compatibility triangles in the system BaO-½Y_2O_3-CuO_x, 950°-1000° Intersecting dashed lines represent change in equilibria from 1:2:1-$BaCuO_{2+x}$ to 3:1:2-2:1:3-Liq at the solidus. •-compounds, o-some of the experimental compositions.

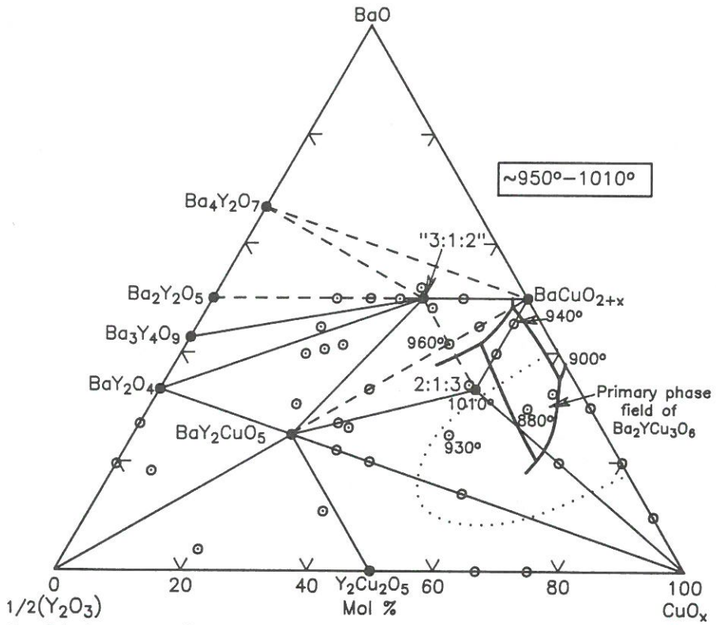

Figure 5 Preliminary melting data in air for part of the system BaO-½Y_2O_3-CuO_x, superimposed on Figure 4, showing best effort at depicting the primary phase field of $Ba_2YCu_3O_{7-x}$. Temperatures listed represent solidus values.

950°C SUBSOLIDUS PHASE DIAGRAM FOR Y_2O_3-BaO-CuO SYSTEM IN AIR

G. Wang, S.-J. Hwu, S. N. Song, J. B. Ketterson, L. D. Marks, K. R. Poeppelmeier, and T. O. Mason
Northwestern University, Materials Research Center, Evanston, Illinois 60201

ABSTRACT

The 950°C subsolidus phase relationships in the Y_2O_3-BaO-CuO system in air were determined by a combination of optical microscopy, X-ray diffraction, and diamagnetic susceptibility measurements. The existence of the binary Ba_2CuO_3 compound was confirmed. Three ternary compounds occur: Y_2BaCuO_5, the ≥90K superconducting $YBa_2Cu_3O_{7\pm\delta}$, and a newly identified compound with Y:Ba:Cu ratio of 1:3:2. A complete solid solution exists between Ba_2CuO_3 and the 1:3:2 compound. Only $YBa_2Cu_3O_{7\pm\delta}$ is superconducting under the preparation conditions employed.

INTRODUCTION

In a recent communication we reported a partial 950°C subsolidus phase diagram for the Y_2O_3-BaO-CuO system in air.[1] A similar partial diagram[2] and a more complete diagram[3] have since been reported. Our partial diagram in Fig. 1 shows the principal join connecting the "green" insulating Y_2BaCuO_5 compound initially reported by Michel and Raveau[4] and the superconductor which has a Y:Ba:Cu ratio of 1:2:3. Our hydrogen reduction thermograms agree with the earlier work of Cava et al.[5] and the neutron diffraction structural refinement of Beno et al.[6] which place the overall stoichiometry at $YBa_2Cu_3O_{7\pm\delta}$. Throughout this paper these two principal phases will be referred to by their appropriate Y:Ba:Cu ratios of 2:1:1 and 1:2:3, respectively.

The 2:1:1-1:2:3 join is particularly significant, since it was very near this join that the initial ≥90K superconducting

assemblage was produced.[7] This composition is circled in Fig. 1. At equilibrium this composition should be approximately biphasic, with 70% 2:1:1 and only 30% superconductor (1:2:3), as was in fact reported in the early studies.[5] Assuming Chu and coworkers were exploring the K_2NiF_4 line in Fig. 1 in search of analogues to the 30-40K superconductors in the La-(Ba,Sr)-Cu-O systems[8], they were extremely fortunate to locate any superconducting compositions. The shaded region in Fig. 1 represents the only compatibility triangles where some fraction of superconducting phase should occur. Within this region, only assemblages with sufficient 1:2:3 phase to ensure interconnectivity between particles will be superconducting.

As we pointed out in our previous communication, the magnetic susceptibility is a much more sensitive indication of the presence of superconducting phase. The closed circles in Fig. 1 indicate where a diamagnetic signal was detected whereas the open circles indicate were no such signal was obtained. It can be seen that the diamagnetic signal intensity persists up to the 2:1:1-CuO join, thus confirming the existence of this subsolidus compatibility.

In the present communication we present the results of our more conventional phase diagram studies resulting in the complete 950°C subsolidus diagram. Once again we have chosen to plot compositions as $YO_{1.5}$-BaO-CuO to correspond with the cation ratios in the ternary compounds obtained. As was shown in Fig. 1, lines representing the layered perovskite structures discussed by Michel and Raveau[9] will be horizontal on such a representation.

EXPERIMENTAL

Compositions in the phase diagram (see Table I) were prepared by solid state reaction of Aldrich yttrium oxide (99.99%), cupric oxide (99.999%), and barium carbonate (99.999%). Guidance for the firing times and temperatures were found in Refs. 9-11. Samples were precalcined at 850-900°C for 8h followed by firing at 950°C in air for an additional 16-40h.

During this time samples were removed from the furnace and reground at least twice to facilitate the reaction. For compositions in the CuO-1:2:3-$BaCuO_2$ triangle melting and/or decomposition was observed at 950°C. These compositions are therefore reported for 850°C and are so indicated in Table I.

Powder X-ray diffraction (XRD) patterns were recorded with Cu K_α radiation using a Ni filter on a Rigaku diffractometer. For reference, patterns of the end-members, all binary compounds, and all ternary compounds were also collected. These agreed well with literature patterns (4,5,9-11). The patterns for the 1:3:2 and Ba_2CuO_3 compounds are given in tabular form in Tables II and III.

Finely ground portions of each composition were immersed in oil and examined via transmitted light optical microscopy. This technique is particularly useful in this system. CuO, $BaCuO_2$, Ba_2CuO_3, 1:2:3, and 1:3:2 are all optically opaque. The opaqueness of the latter two compounds arises from the presence of copper in more than one valence state. $Y_2Cu_2O_5$ is bluegreen while 2:1:1 is distinctively green, and both of these phases are birefringent. In addition, BaY_2O_4, Y_2O_3 and unreacted $BaCO_3$ are clear transparent phases. $BaCO_3$ is strongly birefingent whereas BaY_2O_4 and Y_2O_3 are not. The remaining Ba-Y-oxides are not stable in humid air at room temperature (see Ref. 11) and appear to react to yield opaque products under the optical microscope.

In the BaO-rich portion of the diagram bounded by the 2:1:1-BaY_2O_4 join and the 2:1:1-$BaCuO_2$ join reactions were extremely sluggish. Slow reaction kinetics have already been reported for the Ba-Y-oxides.[11] To accelerate reactions, 0.5 weight percent Li_2CO_3 as a mineralizer was employed in all compositions within the region just specified. This resulted in complete reactions and extremely sharp X-ray patterns for the binary and ternary compounds obtained.

RESULTS AND DISCUSSION

Individual experiments and experimental observations are catalogued in Table I. The data for the open and closed circles

on Fig. 1 are given in Ref. 1 along with the susceptibility results. The closed triangles in Fig. 2 correspond to the compositions in Table I. The diagram will be discussed in couterclockwise fashion beginning with the 2:1:1-$BaCuO_2$ join. Table I also follows this general sequence.

The single point within the CuO-1:2:3-$BaCuO_2$ triangle was necessary to confirm that no additional ternary compounds existed in this region. As pointed out above, this composition and the composition along the 1:2:3-$BaCuO_2$ join could not be fired above 850°C without melting and/or decompostion.

Hinks et al.[2] indicated that no compatibility existed between the 2:1:1 and $BaCuO_2$ compounds due to the presence of additional peaks in compositions fired near this join. It appears that their 6h firing may have been too short or their 1000°C temperature too high to achieve these two compounds, and that the 1:3:2 compound may have been appearing in their patterns. Our two compositions along the 2:1:1-$BaCuO_2$ join clearly establish this compatilibity. Furthermore, as a test, 1:2:3 and 1:3:2 compound powders were reacted at a 50:50 mixture with the result being the 2:1:1 and $BaCuO_2$ phases.

All compatibilities involving the 1:2:3 compound were established in our previous study[1] by XRD, optical microscopy, and susceptibility measurements, as was the $Y_2Cu_2O_5$-CuO-2:1:1 triangle. The $Y_2Cu_2O_5$-2:1:1 join was confirmed in the present study by a reaction at the point indicated on the diagram.

Powder color was diagnostic in the $Y_2Cu_2O_5$-Y_2O_3-BaY_2O_4 portion of the diagram. Colors range from bright green near the 2:1:1 compound to bluegreen near $Y_2Cu_2O_5$ to lighter tints of green as white powders (Y_2O_3, BaY_2O_4) are mixed with the colored phases. This confirms the XRD results which indicate that all tie lines radiate from the 2:1:1 phase in this corner of the diagram.

Some fraction of the birefringent, green 2:1:1 compound could be confirmed by XRD and/or optical microscopy for compositions within the shaded area of Fig. 3. This strongly supports the tie lines as drawn. With the exception of the

CuO-1:2:3-$BaCuO_2$ traingle and the region bounded by $Ba_2Y_2O_5$, $BaCuO_2$, and BaO ($BaCO_3$), the 2:1:1 compound was found in every assemblage.

Three Ba-Y-oxides were detected in our reaction products. Kwestroo et al.[11] reported that although BaY_2O_4 and $Ba_3Y_4O_9$ are the stable phases at high temperature (1300°C), $Ba_2Y_2O_5$ could also be formed at 900°C. This compound subsequently decomposed at 1000°C in favor of yet another compound, $Ba_4Y_2O_7$. Frase et al.[3] report only BaY_2O_4 and $Ba_4Y_2O_7$ in their diagram. It is possible that the mineralizer in the present study served to stabilize the $Ba_2Y_2O_5$ compound which might not otherwise form at 950°C. The coexistence of the three Ba-Y-oxide phases is not inconsistent with the binary phase equilibria sketched out by Kwestroo et al.[11] for this temperature range. It should be remarked at this point that the 12h firing times reported by Frase et al.[3] seem to be too short to have achieved equilibrium without the action of a mineralizer.

The major differences between the diagram of Frase et al.[3] and the diagram in the present study are in the BaO corner. Frase et al.[3] show tie lines radiating from $Ba_4Y_2O_7$ to $BaCuO_2$ and two previously unreported Ba-Cu-oxides with approximate stoichiometries, Ba_2CuO_3 and Ba_3CuO_4. We saw no evidence of a compound at a Ba:Cu ratio of 3:1. However, Ba_2CuO_3 was readily produced and a table of lattice spacings and relative intensities is given in Table II. Between this compound and BaO only Ba_2CuO_3 and unreacted $BaCO_3$ were detected. The Ba_2CuO_3 pattern is quite similar to the pattern for Sr_2CuO_3[12], allowing for tetragonal rather than orthorhombic symmetry.

There appears to be extensive solid solubility along the join connecting Ba_2CuO_3 and the 1:3:2 compound. This was confirmed by preparing undoped (Li-free) compositions across the solid solution at 950°C. Single phase materials were achieved at all compositions in the $Ba_{4-y}Y_yCu_2O_x$ system except for the y=0 end by repeated grinding and firing for times up to one week. Compositions with $y \leq 1/3$ are tetragonal whereas compositions with $y > 1/3$ are orthorhombic. It should be noted

that the Ba_2CuO_3 compound could not be produced without Li_2CO_3 mineralizer. Furthermore, attempts to produce Ba_2CuO_3 without Li_2CO_3 resulted in partial melting at 950°C. The ability of Frase et al.[3] to stabilize the Ba_2CuO_3 compound without mineralizer may have to do with the low purity of their precursors. The structural aspects of the $Ba_{4-y}Y_yCu_2O_x$ solid solution will be the subject of a later communication.

The join connecting BaO with the 1:3:2 compound was confirmed by the persistence of unreacted $BaCO_3$ in all reaction products in the two compatibility triangles involving BaO. As pointed out above, $BaCO_3$ is transparent and strongly birefringent. Although $BaCO_3$ readily reacts with CuO and Y_2O_3 to form the binary and ternary compounds, excess $BaCO_3$ can be expected to remain after firing, given its extremely high decomposition temperature.

To date only the 1:2:3 compound has been found to be superconducting under any set of preparation conditions. This is surprising, given the structural similarity between the Ba_2CuO_3-1:3:2 series and the 1:2:3 compound. Both are layered perovskite derivatives. Additional studies of the $Ba_{4-y}Y_yCu_2O_x$ system are in progress.

Some final comments must be made about the role of Li_2CO_3 in the phase relationships and on superconductivity. A successful mineralizer will promote reaction to the stable phases without altering the phase relationships. To date, all attempts to achieve the pure phases on the diagram (except for Ba_2CuO_3) without mineralizer but with longer reaction times have been successful. The incorporation of Li^+ into the various phases and concomitant alteration in solution thermodynamic properties cannot be completely ruled out.

The Li_2CO_3 resulted in extremely sharp X-ray patterns indicative of high phase purity and excellent crystallinity. This suggested the use of mineralizer in the production of the superconducting phase. Again, very sharp X-ray lines of the orthorhombic phase were obtained. The diamagnetic signal intensity was severely diminished, however, and T_c was reduced

to 75K. High resolution electron microscopy indicated good phase purity as compared with an unmineralized specimen, however there were subtle differences in the images obtained. Whether the destruction of the superconductivity on introducing $LiCO_3$ is related to solid solution effects or other structural factors is a subject of ongoing research.

ACKNOWLEDGMENTS

This work was performed by the Oxide Superconductor Thrust Group of the Northwestern University Materials Research Center with the support of the N.S.F.-M.R.L. program, grant no. DMR-8520280. Helpful discussions with A. J. Freeman and D. L. Johnson are gratefully acknowledged.

REFERENCES

1. S. -J. Hwu, S. N. Song, J. B. Ketterson, T. O. Mason, and K. R. Poeppelmeier, Commun. Am. Ceram. Soc., in press.

2. D. G. Hinks, L. Soderholm, D. W. Capone II, J. D. Jorgensen, I. K. Schuller, C. U. Segre, K. Zhang, and J. D. Grace, submitted to Appl. Phys. Lett.

3. K. G. Frase, E. G. Liniger, and D. R. Clarke, submitted to Commun. Am. Ceram. Soc.

4. C. Michel and B. Raveau, J. Solid State Chem., 43, 73 (1982).

5. R. J. Cava, B. Batlogg, R. B. van Dover, D. W. Murphy, S. Sunshine, T. Siegrist, J. P. Remeika, S. Zahurak, and G. P. Espinosa, Phys. Rev. Lett., 58, 1676 (1987).

6. M. A. Beno, L. Soderholm, D. W. Capone II, J. D. Jorgensen, I. K. Schuller, C. U. Segre, K. Zhang, and J. D. Grace, submitted to Appl. Phys. Lett.

7. M. K. Wu, J. R. Ashburn, C. J. Tong, P. H. Hor, R. L. Meng, L. Gao, Z. J. Huang, Y. Q. Wang, and C. W. Chu, Phys. Rev. Lett., 58, 908 (1987); P. H. Hor, L. Gao, R. L. Meng, Z. J. Huang, Y. Q. Wang, K. Forster, J. Vassilious, C. W. Chu, M. K. Wu, J. R. Ashburn, and C.-J. Torng, Phys. Rev. Lett., 58, 911 (1987).7).

8. H. Takagi, S. -I. Uchida, K. Kitazawa, and S. Tanaka, Jpn. J. Appl. Phys. Lett., preprint.nt.

9. C. Michel and B. Raveau, Rev. Chim. Min., 21, 407 (1984).

10. M. Arjomand and D. J. Machin, J. C. S. Dalton, 1061 (1975).

11. W. Kwestroo, H. A. M. van Hal, and C. Langereis, Mat. Res. Bull., 9, 1631 (1974).

12. C. L. Teske and H. Muller-Buschbaum, Z. Anorg. Allgem. Chem., 371, 325 (1969).9).

Table I
X-ray, Color, and Optical Microscopy Results

Composition Y	Ba	Cu	XRD†‡	Color	Optical Microscopy†
11	44.5	44.5	M-BC, 2:1:1	black	M-opaque m-green
14	43.5	43.5	M-BC, 2:1:1	black	M-opaque m-green
8	42	50*	M-1:2:3, BC	black	opaque
5	30	65*	M-1:2:3, C, BC	black	opaque
50	10	40	M-2:1:1, YC t-?	bluegreen	M-blue, green
70	5	25	M-Y, YC m-2:1:1	bluegreen	M-blue, green, transparent
60	20	20	M-2:1:1 m-Y	green	M-green m-transparent
75	20	5	M-Y, BY_2 m-2:1:1	light green	M-transparent m-green
60	30	10	M-BY_2, 2:1:1	light green	M-green, transparent
54	37	9	M-BY_2, 2:1:1 t-BY	dirty green	M-transparent m-green
45	45	10	M-BY m-1:3:2	dark ash	M-transparent m-green, opaque
40	40	20	M-2:1:1, 1:3:2 t-BY	black/green	M-opaque, green m-transparent
22	56	22	M-2:1:1, 1:3:2, BY	black	M-opaque,transp. m-2:1:1
35	40	25	M-1:3:2, 2:1:1 m-BY	black	M-opaque, green m-transparent
30	40	30	M-1:3:2, 2:1:1	black	M-opaque, green
20	43	37	M-1:3:2, BC m-2:1:1	black	M-opaque m-green
10	50	40	M-1:3:2, BC	black	opaque t-green
33	50	17	M-1:3:2, BY m-2:1:1	black	M-opaque,transp. m-green
25	50	25	M-1:3;2 t-BY	black	M-opaque m-transparent t-green

Y	Ba	Cu	XRD†‡	Color	Microscopy†
34	56	10	M-BY, 1:3:2	black	opaque t-transparent
30	60	10	M-BY, 1:3:2	black	opaque t-transparent
20	70	10	M-B_4Y_2, 1:3:2, bc	black ash	M-opaque m-transp.(b)††
10	80	10	M-bc m-1:3:2, B_4Y_2	black ash	M-transp.(b)†† m-opaque
10	65	25	M-1:3:2 m-B_4Y_2 t-bc	black	M-opaque m-transp.(b)††
5	70	25	M-SS m-bc	black	M-opaque m-transp.(b)††
5	56	39	M-SS m-BC	black	opaque
8	59	33	M-SS	black	opaque
5	90	5	M-bc	light ash	M-transp.(b)†† m-opaque
--	60	40	M-B_2C, BC	black	opaque
--	80	20	M-B_2C, bc	black ash	M-transp.(b)††, opaque

† M=major, m=minor, t=trace
‡ C=CuO, Y=Y_2O_3, YC=$Y_2Cu_2O_5$, BC=$BaCuO_2$, B_2C=Ba_2CuO_3, BY_2=BaY_2O_4, BY=$Ba_2Y_2O_5$, B_4Y_2=$Ba_4Y_2O_7$, 2:1:1=Y_2BaCuO_5, 1:2:3=$YBa_2Cu_3O_7$, 1:3:2=$YBa_3Cu_2O_7$, SS=1:3:2-Ba_2CuO_3 solid solution, and bc=$BaCO_3$.
* Fired at 850 °C
†† Transparent and birefringent ($BaCO_3$)

Table II
X-Ray Data for Ba_2CuO_3

d (nm)	I/Io
0.810	4
0.4055	19
0.2860	100
0.2331	20
0.2234	6
0.2035	3
0.2020	17
0.1803	10
0.1647	25
0.1434	3
0.1426	7
0.1342	4
0.1275	7
0.1216	4

Table III

X-ray Data for $YBa_3Cu_2O_x$ (1:3:2)

d (nm)	I/Io
0.4120	11
0.4013	5
0.3003	9
0.2913	50
0.2876	100
0.2354	19
0.2057	23
0.2001	15
0.1837	4
0.1670	32
0.1649	16
0.1452	5
0.1434	12
0.1353	3
0.1298	9
0.1269	5
0.1175	5

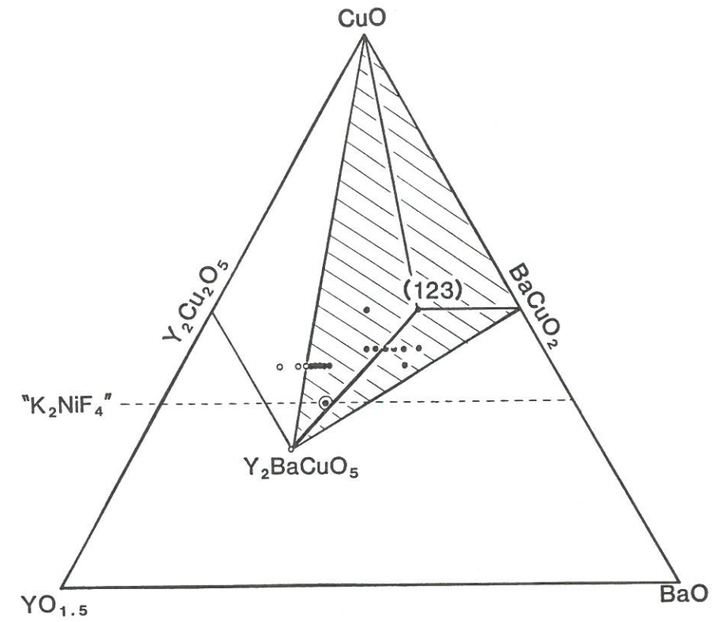

Fig. 1. Partial subsolidus phase diagram for the Y_2O_3-BaO-CuO system at 950°C in air from Ref. 1. The original ≥90K superconducting assemblage of Ref. 7 is circled. The horizontal dashed line indicates the K_2NiF_4 series from Ref. 9. Closed circles indicate where diamagnetic signal intensity was observed. The shaded region indicates where some fraction of the superconducting 1:2:3 compound should occur.

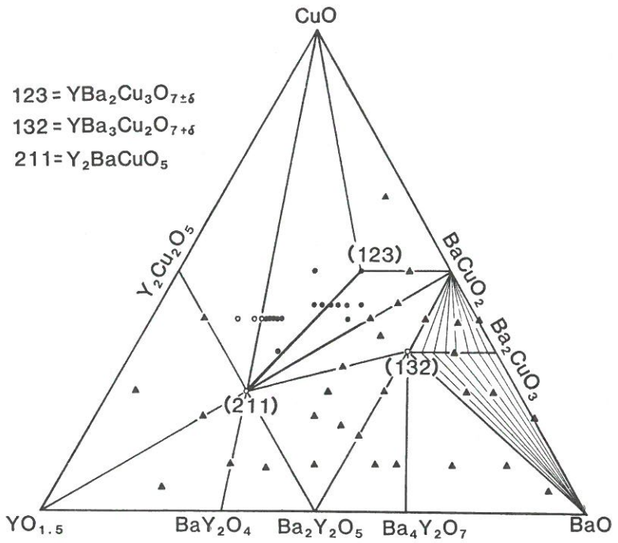

Fig. 2. Complete 950°C subsolidus phase diagram for the Y_2O_3-BaO-CuO system in air. Open and closed circles represent compositions studied by XRD, optical microscopy, and susceptibility (see Ref. 1). Triangles represent the XRD and microscopy work of the present study.

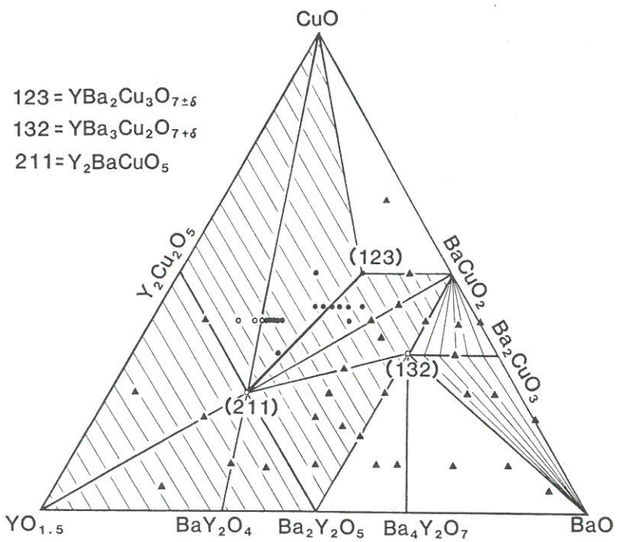

Fig. 3. Same diagram as in Fig. 2 but with regions where the "green" 2:1:1 phase is detected.

Section II

Section II. Processing and Fabrication